

OPERATIONAL EXPERIENCES WITH X-RAY TOMOGRAPHY FOR SRF CAVITY SHAPE AND SURFACE CONTROL*

H.-W. Glock[†], J. Knobloch, A. Neumann, Y. Tamashevich, HZB für Materialien und Energie, Berlin, Germany, J. Kinzinger, XRAYLab, Sachsenheim, Germany, M. Böhnelt, N. Reims, Fraunhofer Institute for Integrated Circuits IIS, Dev. Center X-ray Technology EZRT, Fürth, Germany

Abstract

X-ray tomography has been established as a non-destructive three-dimensional analysis tool, commercially offered by industrial vendors. Typical applications cover shape control and failure detection (voids, cracks) deep inside of complicated bulk pieces like engine blocks, bearings, turbine blades etc.. We evaluated the applicability of the process for superconducting radio frequency cavities, in particular a generic 1.3 GHz single test cell cavity, the 1.4-cell 1.3 GHz bERLinPro electron gun cavity and the 1.5 GHz VSR-1-cell-prototype cavity. The gun cavity experienced severe shape modifications during its tuning process and features a complicated internal stiffening construction. Thus it is a challenge to measure its actual internal cavity surface shape after the complete preparation process with a resolution, sufficiently high (better than 0.2 mm) to serve as input for meaningful comparative field simulations. First tests with a vendor's on-site X-ray source, operating at X-ray energies up to 590 keV revealed an insufficient resolution of the inner surface, attributed to the unfavorable X-ray damping characteristics of niobium. This was overcome with the aid of an accelerator-based source (X-ray spectrum up to 7.5 MeV), operated by Fraunhofer IIS-EZRT, Fürth, Germany. Results show significant, while understood, shape changes and indicate partial inner surface modifications of the gun cavity. Further, the data evaluation process, which was needed to provide input for field simulations, raised issues because of data set size and complexity and illustrated further some typical artefacts, which are discussed in the paper.

typically accomplished by a motor-driven rotation of the test object around a vertical axis, not necessarily central to the object (cf. Fig. 1). Industrial X-ray tomography is used both for the control of shape precision and the non-destructive detection of internal material failures like cracks or voids in bulk and e.g. welded regions. Applications covers a wide variety of technical objects, which are subject of high quality or reliability demands, ranging from e.g. printed circuit boards and connector plugs, compound materials, entire engine blocks up to damage analysis in full-size crashed cars [1].

To the best of author's knowledge the first application of X-ray tomography to superconducting accelerating cavities was described in Ref. [2], there applied to a 3.9 GHz 9-cell cavity with a reported Nb wall thickness of less than 1 mm. The authors added their own experimental experiences in Ref. [3], with the aim to determine the actual cavity shape of a 1.4 cell SRF electron gun cavity, operated at 1.3 GHz and with Nb wall thickness of ~ 3 mm, after a complicated tuning process. In this study the tomographic inversion failed to determine the inner cavity contour, which was attributed to the strong specific X-ray damping of Nb. In order to overcome this the X-ray energy was increased up to 7.5 MeV (instead of 590 keV in the previously used conventional X-ray tube), thus taking profit from lower specific absorption rates [4]. For this purpose the accelerator-driven tomography installation of Fraunhofer IIS-EZRT, Fürth, Germany was used both for the above-mentioned gun cavity, the VSR-1-cell-prototype cavity [5] and a generic single cell 1.3 GHz cavity.

All measurements were done with an X-ray array detector with $N_p \times N_p = 2048 \times 2048$ square pixels of $\Delta p = 200 \mu\text{m}$ edge length, distances of (cf. Fig. 1) $L_1 \approx 5 \text{ m}$, $L_2 \approx 0.5 \text{ m}$, resulting in a maximum object size (perpendicular to the detector) of ~ 372 mm. This led to some truncations of peripheral areas, which were minimized by careful positioning. The electron accelerator (a Siemens SILAC®-p 9 MeV) delivers a beam spot size of $\Delta s < 2 \text{ mm}$ on a tungsten target. Both the finite size of each detector element and of the X-ray source area limit the accuracy Δd of the transversal position, which later on is attributed to a certain material compartment of the test object, given by (cf. [6], Equation (10), using our nomenclature):

$$\Delta d = \frac{\sqrt{[L_2 \Delta s]^2 + [L_1 \Delta p]^2}}{L_1 + L_2} \quad (1)$$

TOMOGRAPHY SETUP

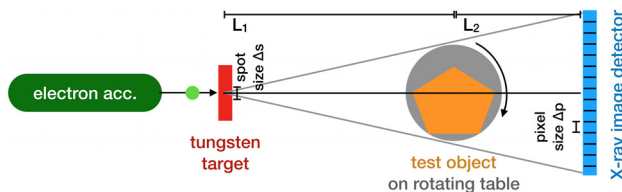


Figure 1: Schematic set-up for X-ray tomography.

X-ray tomography is essentially based on an inversion algorithm capable to derive the three-dimensional material distribution of the test object out of a large set of X-ray transmission pictures, each captured in a different angle of transmission through the test object. This is

* Work supported by German Bundesministerium für Bildung und Forschung, Land Berlin, and grants of the Helmholtz Association

[†] hans.glock@helmholtz-berlin.de

Content from this work may be used under the terms of the CC BY 3.0 licence (© 2019). Any distribution of this work must maintain attribution to the author(s), title of the work, publisher, and DOI

This results with the data given above in a transversal uncertainty of $\Delta d = 257 \mu\text{m}$. Typically details down to half that size may be resolvable in the tomographic results, as far as geometric relations between the source, the rotation axes of the test object and the detector are kept stable during the capturing process with according precision.

TOMOGRAPHY DATA EVALUATION

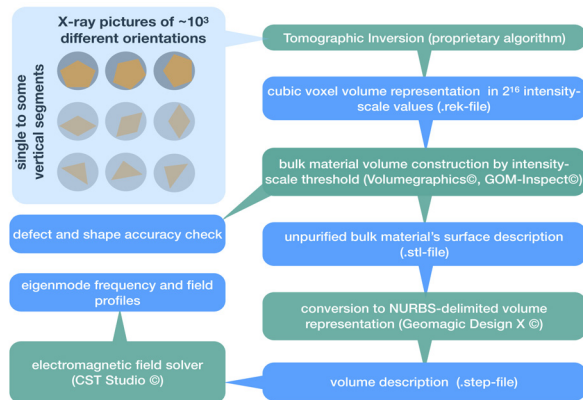


Figure 2: Data evaluation process

The data evaluation process is illustrated in Figure 2. A large set (typically 1500 to 3600) of X-ray transmission pictures, subsequently taken with small identical angular increments, and – in case of objects exceeding the detectors height – possibly some sets of different vertical ranges, are fed into the tomographic inversion algorithm. Even though this is the core element of the entire process, it is considered here as a black box instance, both because of the underlying complexity as being subject of more than a single field of mathematical theory, and not being central for the discussion of the application. It is sufficient to understand the tomography’s direct output as a three-dimensional array of an intensity-scale value (typically of two byte value range) expressing the calculated specific X-ray absorption for each cubical voxel in a cubical box of $N_p \cdot \Delta p \cdot L_1 / (L_1 + L_2)$ corner length. The voxel size Δv is not directly correlated to the detector’s pixel size but is, within its limits, a matter of choice, typically not smaller than $\Delta d/2$ (in our case $\Delta v = 180 \mu\text{m}$). Such voxel data sets, even though of simple structure (but of rather unhandy size of several GBytes) are of limited direct usability, since detailed inspection and, even more, further numeric evaluation demand for more sophisticated navigational means than pure slicing perpendicular to coordinate axes. Figure 3 shows such a slice together with a histogram of all intensity-scale values found in the tomography output. The definition of the threshold (also pictured there) is a crucial step of the process, especially if the tomography resulted in noisy areas. This is likely to happen if in a significant portion of single captures the according areas are shadowed by other absorptive volumes. Therefore the threshold is still routinely adjusted manually in order to balance between noisy surfaces (threshold too low) and holes in thin walls (too high).

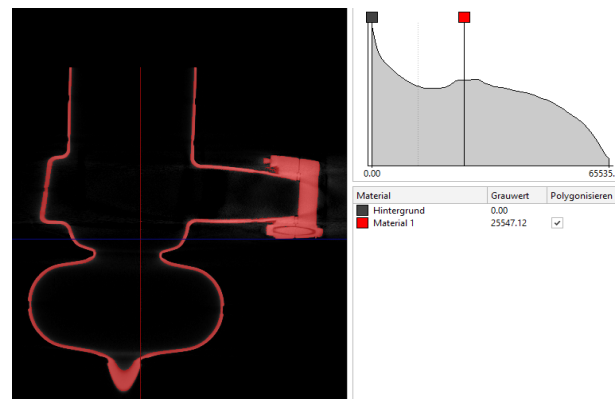


Figure 3: Single slice of tomography-computed intensity-scaled specific X-ray absorption. The VSR-1-cell prototype cavity was intentionally tilted against the axis of rotation, which causes the misleading impression of unexpected shape distortions. The vertical line in the histogram indicates the threshold, above which voxels are attributed as solid metal, whereas such below are accounted as free space.

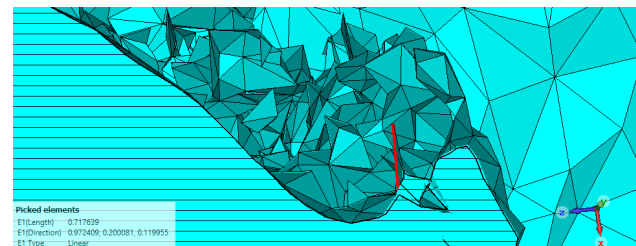


Figure 4: Detail of the VSR-1-cell cavity wall in a noisy region, imported per STL into CST. The triangle with the edge marked in red (of length of 0.72 mm) is a pure surface element, not delimiting a volume.

Once voxel sets of bulk material zones are separated from those of empty space, dedicated software tools are needed to form a geometric entity describing the bulk cavity shell. The authors routinely use VolumeGraphics© [7] and also found GOM-Inspect© [8] as a cost-free alternative for pure inspection and shape control. Both programs offer the ability to export a triangulated surface of the cavity volume (N. B. not its interior, but its wall) in the widely popular STL-format. Even though it was possible to import and display such files into CST© [9], only the hexahedral mesher was capable to generate a mesh; sufficient for wakefield computations, but not well suited for eigenmode computations under high geometrical precision demands. Analysis of the STL datasets showed a non-negligible amount of surface errors like holes, triangles, which are not or only partially connected, and typically several hundreds of small separate “hovering” volumes in those areas, where the material boundary quality is poor, caused by a weak contrast in the tomography’s result (cf. Fig. 4).

Searching for a tool capable to reduce the noisy local surface complexity while keeping the parameters of the smooth shape with high precision, and also providing a data transfer format compatible to popular field solvers, we found to our best knowledge the only working

Content from this work may be used under the terms of the CC BY 3.0 licence (© 2019). Any distribution of this work must maintain attribution to the author(s), title of the work, publisher, and DOI

solution in GeoMagic Design X © [10]. This software is intended to reverse-engineer geometrical 3-D scan data from various kind of sources, to correct data errors both automatically and by user control and to identify geometrical elements typical in technical objects or – of highest relevance in our application – to describe scanned geometries segment-wise by non-rational uniform B-spline (NURBS) surfaces. Those are basic elements of STEP-formated volume descriptions and thus compatible e.g. with CST©.

OUTCOMES OF X-RAY TOMOGRAPHIC INSPECTIONS

Structure Integrity Analysis

X-ray inspections are well established for checking the integrity of bulk material and mating zones like welds (cf. Fig. 5), whilst typically restricted to a few perspectives. Tomography adds full volume information, but also may reduce the contrast of material surfaces in case of difficult transmission conditions. Furthermore it is possible to gain insight from otherwise inaccessible areas (cf. Fig. 6)

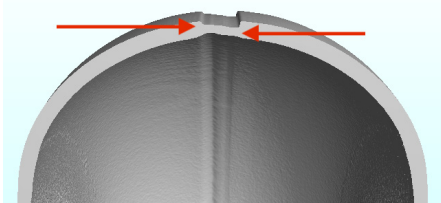


Figure 5: Equator weld of the generic single cell cavity showing a noticeable radial offset.

Shape Control

Because of the paramount meaning of shape precision control in several fields of technology, dedicated software to comfortably compare design and measured geometries is available. Such a comparison is shown in Fig. 7 for the VSR-1-cell-prototype cavity, illustrating a nicely matching waveguide coupler section and attached half cell, whereas significant deviations up to 2 mm are seen on the outer half cell. This need not be attributed to a failure but is likely the result of the half-cell-trimming and tuning process.

Input for Field Simulation

Tomography offers a mean to measure a cavity shape after the entire preparation and tuning process even under vacuum, allowing for computation of mode frequencies and field profiles for the actual shape, instead of the design, which, to our best knowledge, is the first time demonstrated here (cf. Fig. 8). The computed frequency of 1478.184 MHz has to be compared with a measured value of 1476.979 MHz (air filled, 23°C, 40 % rel. hum, normal pressure), corresponding to 1477.439 MHz with $\epsilon_r = \mu_r = 1.0$. That results in a relative error of $0.504 \cdot 10^{-4}$, corresponding to 92 μm , based on 183 mm inner cell diameter.

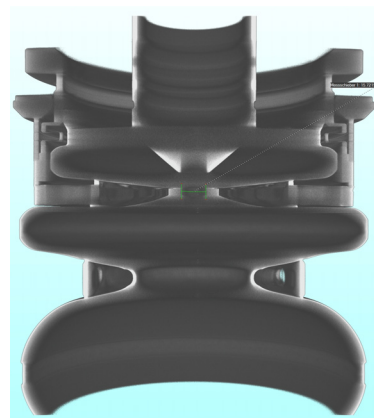


Figure 6: Tomography cross section of the Gun 1.1 cavity illustrating the capability to gain geometrical information from deep inside of multi-layered structures; also showing the fading contrast of the innermost parts.

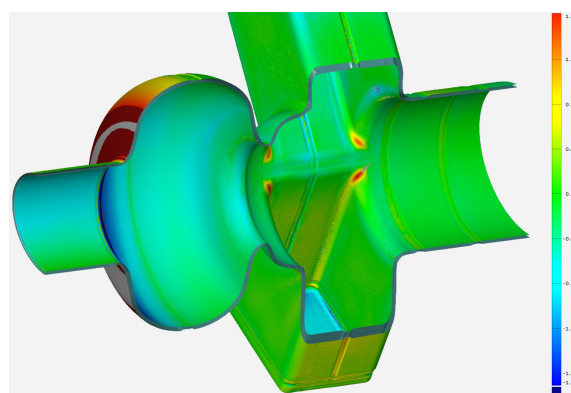


Figure 7: Colour-coded normal distance (in mm) between design and tomographically measured shape; blue indicate a surface inside the design volume, red such above it.

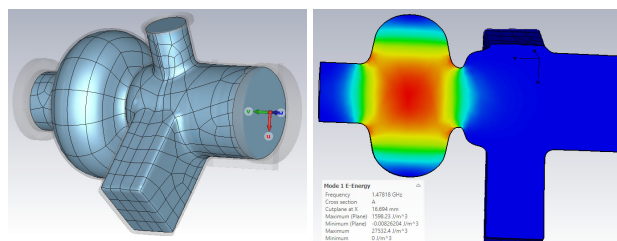


Figure 8: CST© model based on NURBS-imported tomography shape (left) and its fundamental mode.

CONCLUSION

X-ray tomography of Nb cavities opens new possibilities for integrity and especially full-structure shape control on a 0.2 mm precision level. The strong specific X-ray absorption of niobium nevertheless demands for high-energy X-ray sources, only in case of thin walls (less ≈ 1 mm) manageable with electrostatic tubes; otherwise accelerator-based sources are mandatory. Powerful computational resources and highly specific software are needed, especially if data transfer to tools for further physics simulation is intended. Even under those prerequisites user experience is inevitable in order to identify artefacts. The authors plan to broaden this knowledge base with further comparative experiments.

REFERENCES

- [1] M. Sackewitz, Fraunhofer-Allianz Vision., “Leitfaden zur Industriellen Röntgentechnik”, *Fraunhofer Verlag*, Stuttgart, 2. Aufl., 2015, ISBN 978-3-8396-0913-2
- [2] M. Bertucci *et al.*, “Test, diagnostics and computed tomographic inspection of a large grain 3.9 GHz prototype cavity”, in *Proc. 8th Int. Particle Conf. (IPAC'17)*, Copenhagen, Denmark, pp. 1011-1014, doi:10.18429/JACoW-IPAC2017-MOPVA062
- [3] H.-W. Glock *et al.*, “Preparation and Testing of the bERLinPro Gun1.1 Cavity”, in *Proc. 9th Int. Particle Accelerator Conf. (IPAC'18)*, Vancouver, Canada, May 2018, pp. 4117-4120. doi:10.18429/JACoW-IPAC2018-THPMF032
- [4] J. H. Hubbell S. M. Seltzer, “Tables of X-Ray Mass Attenuation Coefficients and Mass Energy-Absorption Coefficients 1 keV to 20 MeV for Elements Z = 1 to 92 and 48 Additional Substances of Dosimetric Interest”, *NISTIR 5632*, National Institute of Standards and Technology, Gaithersburg, MD 20899, USA, May 1995, pp. 44-45.
- [5] A.Velez *et al.*, “The SRF Module Developments for BESSY VSR”, in *Proc. 8th Int. Particle Conf. (IPAC'17)*, Copenhagen, Denmark, pp. 986-989, doi:10.18429/JACoW-IPAC2017-MOPVA053
- [6] American National Standard, “Standard Guide for Computed Tomography (CT) Imaging, E1441-97”, *ASTM*, West Conshohocken, PA 19428-2959, USA, pp. 15-16.
- [7] VolumeGraphics VGStudio 3.2, Volume Graphics GmbH, Speyerer Straße 4 – 6, 69115 Heidelberg, Germany.
- [8] GOM-Inspect-2018, GOM GmbH, Schmitzstraße 2, 38122 Braunschweig, Germany.
- [9] Simulia CST Studio Suite Vers. 2019.05, Dassault Systemes Deutschland GmbH.
- [10] Geomagic Design X Vers. 3.2, 3D Systems Corporation, Rock Hill, SC 29730, USA.